EARTHQUAKE ENGINEERING AND STRUCTURAL DYNAMICS, VOL. 26, 1091–1112 (1997)

IN-PLANE SEISMIC RESPONSE OF BRICK MASONRY WALLS

GUIDO MAGENES AND GIAN MICHELE CALVI*
Department of Structural Mechanics, University of Pavia via Ferrata 1, 27100 Pavia, Italy

SUMMARY

The paper addresses the problems of evaluation of strength, deformability, and energy dissipation capacity of unreinforced brick masonry walls, within the context of seismic assessment of existing buildings. Possible approaches to simplified strength evaluation are discussed on the basis of experimental and numerical data, and formulae for assessment are presented. The role of the shear ratio in the shear failure mechanisms is put in evidence and shear strength formulae are proposed accordingly. The most significative parameters regarding deformability under cyclic loading are highlighted and energy dissipation due to hysteretic behaviour is quantified for possible use in dynamic models. Experimental results show how ultimate drift seems to be a parameter with high regularity for walls failing in shear. Based on such result, a possible approach for seismic assessment is outlined. © 1997 John Wiley & Sons, Ltd.

Earthquake Engng. Struct. Dyn., **26**, 1091–1112 (1997)

No. of Figures: 10. No. of Tables: 4. No. of References: 23.

KEY WORDS: masonry; strength; shear; energy dissipation; assessment

1. INTRODUCTION

Unreinforced masonry buildings in seismic zones constitute a hazard which has generated significant interest in the development of appropriate assessment, analysis, and retrofit methods. The large number and variety of these buildings, most of which were constructed before the development of rational engineering design procedures, calls for rational approaches to assessment, well supported and validated by experimental research. This paper outlines some of the critical issues related to the behaviour of simple walls, and proposes some possible approaches, drawing on the experience of past and ongoing research on seismic response of unreinforced masonry structures at the University of Pavia.

Typical Unreinforced Masonry (URM) buildings are likely to be composed of several load-bearing masonry walls arranged in orthogonal planes, with relatively flexible floor diaphragms. Observed seismic damage in URM structures often includes out-of-plane failures of walls, driven by excessive deflections of diaphragms and insufficient connections between them. Once out-of-plane failure is prevented by proper measures (e.g. reinforced concrete ring beams, steel ties at the floor levels ...) the in-plane walls provide the stability necessary to avoid collapse. Usually, these walls are pierced by windows or doors, leaving a series of smaller piers to provide both the gravity and lateral load resisting systems. The behaviour of such URM components differs dramatically from frame-type structures or reinforced concrete structural wall buildings. Mechanisms of lateral force resistance depend primarily on the pier geometry, on their boundary conditions and on the magnitude of vertical loads, and then on the characteristics of the brick, of the mortar and of the brick/mortar interface. Flexural response tends to be dominated by rocking of piers rather than 'beam'-type

* Correspondence to: G. Michele Calvi, Universita degli studi di Pavia, Dipartimento di Meccanica Strutturale, Via Abbiategrasso 211, Pavia 27100, Italy

Contract grant sponsor: CNR

CCC 0098–8847/97/111091–22$17·50

Received 26 July 1996
Revised 18 February 1997

behaviour, and failure is generally characterized by shear, either in a diagonal tension mode or by sliding on the predefined planes of the mortar joints. Furthermore, masonry is sensitive to loading rates, boundary conditions, and the effect of axial loads. The non-homogeneous, composite nature of masonry makes component behavior difficult to predict, and also difficult to replicate in the laboratory.

The main objective of the research presented in this paper is the development of a procedure to assess the response of brick masonry walls, considering their strength and their deformation and energy dissipation capacity. To this end both refined numerical simulations and laboratory tests have been performed. The analysis and interpretation of the results has allowed an improvement in the prediction of strength, failure modes and non-linear response of masonry walls.

It must be stressed that the study presented here was carried out on one particular type of masonry, with materials having almost constant mechanical characteristics, to reduce the scatter of experimental results as much as possible. Since analytical procedures are provided, extension to other masonry material is possible, provided appropriate experimental data are available.

2. STRENGTH OF MASONRY PIERS SUBJECTED TO IN-PLANE LOADING

The principal failure mechanisms of masonry piers subjected to seismic actions can be summarized as follows:

1. *rocking failure*: as horizontal load or displacement demand increase, bedjoints crack in tension, and shear is carried by the compressed masonry; final failure is obtained by overturning of the wall and simultaneuos crushing of the compressed corner.
2. *shear cracking*: peak resistance is governed by the formation and development of inclined diagonal cracks, which may follow the path of bed- and head-joints or may go through the bricks, depending on the relative strength of mortar joints, brick–mortar interface, and bricks.
3. *sliding*: due to the formation of tensile horizontal crack in the bedjoints, subjected to reversed seismic action, potential sliding planes can form along the cracked bedjoints; this failure mode is possible for low levels of vertical load and/or low friction coefficients.

The strength associated to these failure modes can be described simply, sacrificing some accuracy to the purpose of emphasizing the relative importance of various parameters on the response of piers. The following sections will be dedicated to a discussion of the possible approaches to simplified strength assessment.

2.1. Existing simplified formulations

The maximum horizontal shear which can be resisted by a *rocking* pier failing under static in-plane loading may be approximated introducing a proper stress distribution for the masonry in compression and neglecting the tensile strength of bedjoints. With reference to Figure 1, equilibrium leads to the following expression:

$$V_r = \frac{D^2 t}{H_0}\frac{p}{2}\left(1-\frac{p}{\kappa f_u}\right) = \frac{Dt}{\alpha_V}\frac{p}{2}\left(1-\frac{p}{\kappa f_u}\right) \tag{1}$$

where D is the pier length, H_0 is the effective pier height (distance from zero moment), t the pier thickness, $p = P/(Dt)$ is the mean vertical stress on the pier due to the axial load P, f_u is the compressive strength of masonry, κ is a coefficient which takes into account the vertical stress distribution at the compressed toe (a common assumption is an equivalent rectangular stress block with $\kappa = 0{\cdot}85$). The effective height H_0 is determined by the boundary conditions of the wall and is related to the shear ratio α_V:

$$\alpha_V = \frac{M}{VD} = \frac{H_0}{D} = \frac{\psi' H}{D} \tag{2}$$

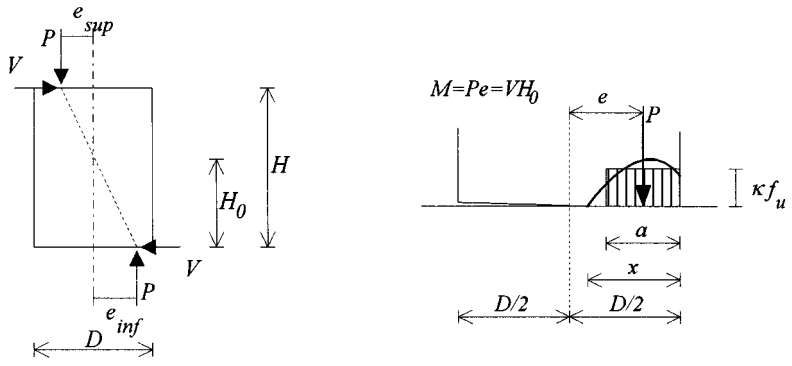

Figure 1. Assumptions for rocking strength evaluation of a wall failing with crushing at the base corner

Considering typical test layouts, the parameter ψ' assumes a value of 1 when the pier is fixed on one end and free to rotate on the other, and a value of 0·5 when the pier is fixed at both ends. It can be seen that equation (1) has a low sensitivity to the parameters κ and f_u, in the range of low mean vertical stresses (i.e. for p/f_u lower than 0·2), while it is strongly affected by the parameter α_V (and consequently by ψ').

The *shear* failure of URM piers associated with diagonal cracking is difficult to describe with a simple expression, since it is the result of several interacting factors, where the heterogeneity of masonry plays a dominant role. The phenomenology of shear failures of unreinforced piers subjected to vertical load and increasing horizontal displacements has been described in several works (References 1–6 among others), and can be strongly influenced by the quality of mortar and bricks. If the attention is restricted to old brick masonry, experiments[1,2] have shown that the onset of visible diagonal cracking can often be associated with the attainment of the peak lateral force after which strength degradation takes place. In some cases a moderate increase in force was measured after the appearence of diagonal cracks, but generally the diagonal cracking load lies between 85 and 100 per cent of the peak shear force.

Two main types of simplified approaches are used for the prediction of shear strength associated to diagonal cracking. One approach was originated from tests performed in Ljubljana (Slovenia)[5,6] on URM piers with doubly fixed boundary conditions ($\psi' = 0{\cdot}5$), and it is based on the assumption that diagonal shear failure is attained when the principal stress at the center of the pier attains a critical value, which is defined as a reference tensile strength of masonry. With such an approach, a shear strength formulation was proposed[4–6] in the form

$$V_d = \frac{f_{tu} D t}{b} \sqrt{1 + \frac{p}{f_{tu}}} \tag{3}$$

where f_{tu} represents the conventional tensile strength of masonry (not to be confused with the tensile strength of bed joints) to be determined by shear tests on wall specimens, and b is a parameter which was assumed to be dependent on the pier aspect ratio H/D, and accounts for the distribution of shear stress at the center of the wall. A value of $b = 1{\cdot}5$ has been proposed for walls with aspect ratio greater than 1·5, a value close to 1·1 has been proposed for walls with aspect ratio equal to 1·0, giving good agreement with experimental results. In Reference 7 a possible criterion for design practice was proposed as: $b = 1$ for $H/D \leqslant 1$, $b = H/D$ for $1 < H/D < 1{\cdot}5$, $b = 1{\cdot}5$ for $H/D \geqslant 1{\cdot}5$. Although the simplification of idealizing masonry as an equivalent isotropic homogeneous continuum is rather drastic, this approach has the main merit of being based on only one parameter, which is the reference tensile strength. The determination of f_{tu} must be based on experiments on masonry panels (shear tests), by inverting equation (3), and in principle only

one test would be sufficient to give an estimate of the parameter f_{tu}. In many instances this approach has given a good prediction of shear strength, although no clear indications and exhaustive experimental references are yet available for the definition of the parameter b for a wide range of aspect ratios and for boundary conditions different from fixed-fixed.

A second approach is based on a Mohr–Coulomb formulation, which can be physically justified especially in the cases where diagonal cracking is associated with mortar bed- and head-joint failure. The criterion is usually formulated in the form of an ultimate shear stress:

$$\tau_u = c + \mu\sigma_v \tag{4}$$

This approach is largely adopted in design and assessment of masonry structures. However, different interpretations have been given in its practical use for the evaluation of the ultimate load V_d of a wall. One approach is to consider τ_u given by equation (4) as the expression of an average ultimate shear stress in the horizontal section of the wall, and to put σ_v equal to the mean vertical stress in the pier, p i.e.:

$$V_d = Dt\,\tau_u = Dt\,(c + \mu p) = Dt\left(c + \mu\,\frac{P}{Dt}\right) \tag{5}$$

It is evident that in this approach the parameters c and μ have the meaning of global strength parameters and cannot be related to local material properties such as the strength parameters of the bedjoints, since the real stress distribution is non-uniform. Another possible approach is to take into account wall cracking due to flexure, and to consider again equation (4) as the expression of an average ultimate shear stress, referred however to the effective uncracked section length. This approach is adopted for instance by the Eurocode 6 on masonry structures.[8] Typically, the length of the effective uncracked section is calculated neglecting the tensile strength of bedjoints and assuming a simplified distribution of compression stresses, most commonly constant or linear. If this latter hypothesis is followed, the effective uncracked section length D' is easily calculated as

$$D' = \beta D = 3\left(\frac{1}{2} - \frac{V}{P}\,\alpha_V\right)D = 3\left(\frac{1}{2} - \frac{V}{P}\,\frac{H_0}{D}\right)D \tag{6}$$

The ultimate shear capacity of a wall can thus be calculated as

$$V_d = \beta Dt\left(c + \mu\,\frac{P}{\beta Dt}\right) = \beta Dt\left(c + \mu\,\frac{p}{\beta}\right) = Dt\left(\frac{1{\cdot}5c + \mu p}{1 + 3\,\dfrac{c\alpha_V}{p}}\right) \tag{7}$$

Also this latter approach does not consider equation (7) as a description of a local failure, and parameters c and μ should be considered as global strength parameters. The choice to make the calculation referring to the cracked section, despite reasonable, does not happen to result in good agreement with the numerous experiments on walls (in particular, those with doubly fixed boundary condition) where diagonal cracking is initiated at the centre of the panel, far from the extreme sections of the piers which are subjected to higher flexural cracking. It may be mentioned that the same 'cracked section' approach is sometimes used in the application of the criterion associated to equation (3). Moreover, further corrections are sometimes introduced in equations (5) or (7) in an attempt to correlate them with a local state of stress and a local failure, taking into account the nonuniform distribution of stresses along a section (e.g. assuming parabolic distribution of shear stresses).

The strength of a pier undergoing *sliding*, under seismic excitation, along a horizontal joint is sometimes expressed as

$$V_s = \mu P \tag{8}$$

where μ represents the sliding coefficient of friction of the masonry joint, and cohesion is neglected invoking the fact the joint is already cracked in tension due to flexure. If the coefficient μ is put equal to the residual friction of a sliding bedjoint, equation (8) tends to underestimate rather significantly the load which corresponds to the *onset* of sliding, since the sliding resistance of a joint cracked in tension is higher than the residual sliding strength of a bedjoint failing in shear. Expressions like equations (5) or (7) could be considered more appropriate than equation (8), if the case with a reduced value for the cohesion.

2.2. *Numerical simulation of shear strength of panels and proposed shear strength formulae*

Recent developments in analytical modelling have provided the possibility for investigating some aspects of shear failure. A constitutive model recently developed for solid brick masonry by Gambarotta and Lagomarsino[9,10] has been implemented for the purpose of this study in the finite element code ADINA.[11] The model was calibrated mostly on experiments performed within a recent research program on unreinforced masonry carried out in Italy.[1,12,13] The model describes masonry as a layered material, whose properties are derived from brick and joint properties via a homogenization procedure. Scalar damage variables are used to reproduce the following fundamental mechanisms: opening of bedjoints, sliding of bedjoints, shear failure of bricks and crushing of masonry in compression. The model showed an excellent ability to simulate the behaviour of brick masonry with weak mortar joints, as common in old buildings, and was used here to obtain an indication on the strength mechanisms of simple walls by simulating shear-compression tests with different combinations of mechanical parameters (namely cohesion c and friction μ of the bedjoints), different levels of axial load and different boundary conditions (fixed–fixed or cantilever tests), different aspect ratios of the walls, for a total of 33 simulated tests dominated by shear failure. The ranges of variation of the parameters were: cohesion of bedjoints $c = 0{\cdot}09$–$0{\cdot}4$ MPa, friction coefficients $\mu = 0{\cdot}4$–$0{\cdot}8$, mean stress $p = 0{\cdot}2$–$1{\cdot}0$ MPa ($p/f_u \cong 0{\cdot}025$–$0{\cdot}17$), aspect ratio $H/D = 0{\cdot}48$–$2{\cdot}0$, shear ratio $\alpha_V = 0{\cdot}24$–1.

A first useful observation which could be drawn from the numerical simulation regards the evolution of mortar joint damage in correspondence of the peak strength of walls. In the constitutive model, a value of the dimensionless damage scalar parameter α_m equal to 1 correspond to the attainment of the peak strength of the joint either in shear or in tension. Values of α_m greater than unity correspond to the strain-softening regime (i.e. 'cracked') state, while values lower than unity correspond to the uncracked state. Damage in the mortar joints is always present at the sections with the highest moment, and is due to crack opening and limited local shear sliding, early before the attainment of the peak strength. This damage typically propagates in a stable and slow fashion, until a sudden and unstable propagation occurs, which determines the failure of the wall and initiates the softening branch of the load–displacement curve. In the finite element analyses, attention was paid to the damage propagation at peak lateral force during the simulated shear tests (between points A and B of Figure 2). The unstable propagation of cracks could be localized in the joints of the extreme sections which were subjected also to flexural cracking (case I of Figure 2), or could be initiated at the center of the panel, where no flexural cracking was present (case II of Figure 2), or, in an intermediate mechanism, could be along a diagonal direction of shear damage zones, which from the extreme sections join through the centre of the panel. These phenomena show how a proper approach to the evaluation of shear strength with simplified formulations should consider both a 'cracked section' approach, proper of the extreme sections cracked in flexure, and a 'whole section' approach, which seems appropriate for the central zones of the walls, in a double bending condition.

The second observation which could be derived was on the influence of the aspect ratio (H/D) or the shear ratio ($\alpha_V = M/(VD) = H_0/D$). It is known from experiments that the mean shear strength of walls increases as the wall gets squatter, but since the experimental tests are usually made with only one type of boundary conditions, aspect ratio and shear ratio vary in the same proportion. As a consequence, some strength formulae introduce a correction factor based on the aspect ratio, while in other formulae the shear ratio is used. The numerical simulations could easily allow the change of boundary conditions, and the results showed that the dominating factor is the shear ratio α_V. Keeping all other parameter constant, the mean

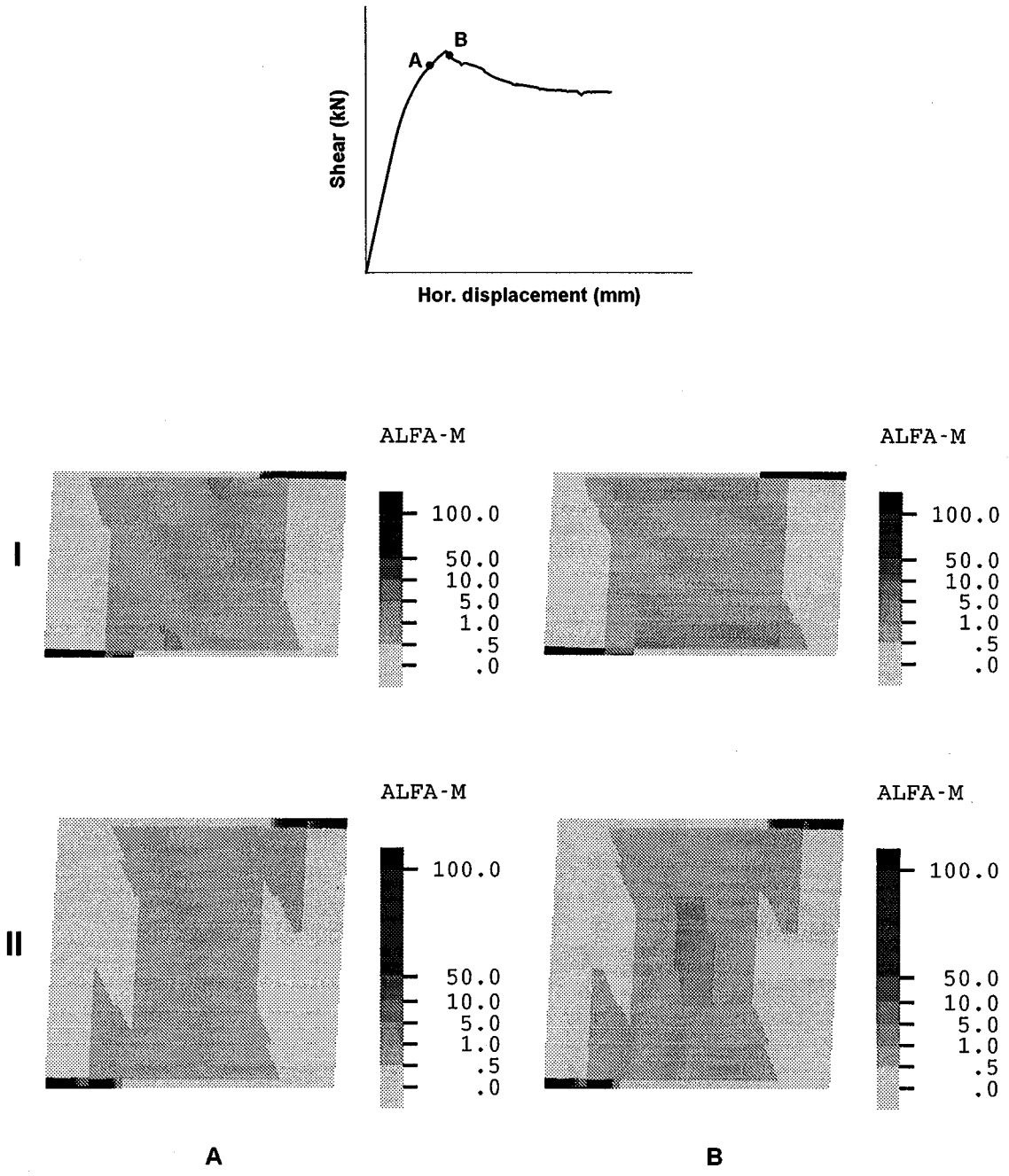

Figure 2. Non-linear finite element analyses: distribution of the bedjoint damage parameter α_m before (A) and immediately after (B) the attainment of the peak shear strength. Case I: failure mechanism in proximity of the sections with highest flexural cracking. Case II: failure mechanism initiated at the centre of the wall

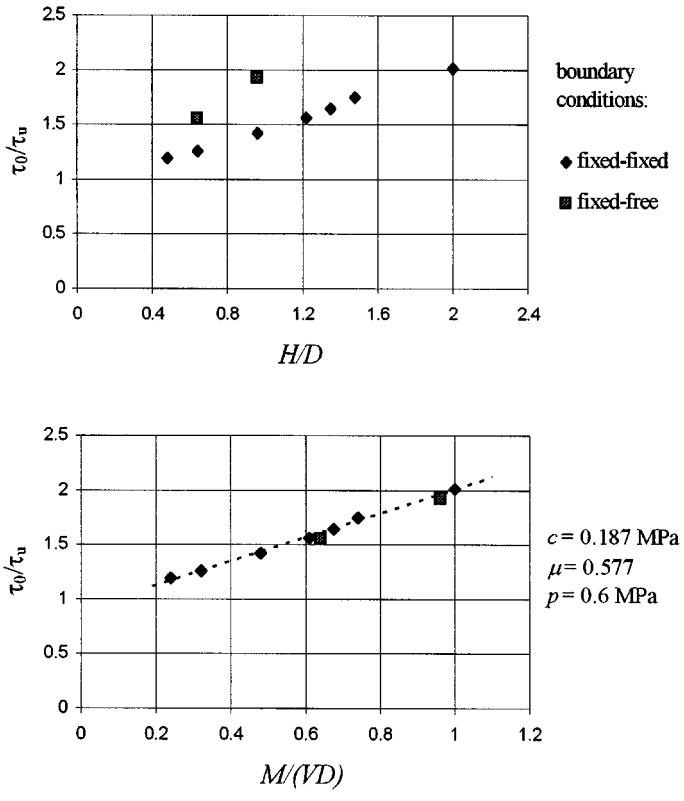

Figure 3. Influence of aspect ratio and shear ratio on shear strength of masonry walls from f.e.m. simulations; $\tau_0 = c + \mu p$, $\tau_u = V_u/Dt$, V_u peak strength from finite element simulation

shear strength $\tau_u = V_d/(Dt)$ decreased hyperbolically as the shear ratio increased, or, in a simpler way, the reciprocal of τ_u increased linearly with the shear ratio, as shown in Figure 3. Such influence of the shear ratio was apparently not influenced by the type of damage propagation. An appropriate simplified strength formulation could thus reflect such influence with a correction factor which is a linear function of α_V. A simple approach could be as follows:

$$V_d = Dt\,\tau_u \quad \text{with } \tau_u = \min(\tau_{cs}; \tau_{ws}) \tag{9a}$$

$$\tau_{cs} = \frac{1{\cdot}5c + \mu p}{1 + 3\,c\alpha_V/p} \quad \text{relevant to the cracked section} \tag{9b}$$

$$\tau_{ws} = \frac{c + \mu p}{1 + \alpha_V} \quad \text{relevant to the whole section} \tag{9c}$$

where equation (9b) is directly taken from equation (7). By using the same values for c and μ which were used in the constitutive model for the finite element analyses, the strength criterion given by equation (9) would give the results shown in Figure 4. Given the simplicity of the formulation, the results are satisfactory when compared to the results of the finite element simulations, giving errors of less than 10 per cent. Also, good agreement with the observed damage propagation was found, i.e. equation (9b) governed for cases similar to

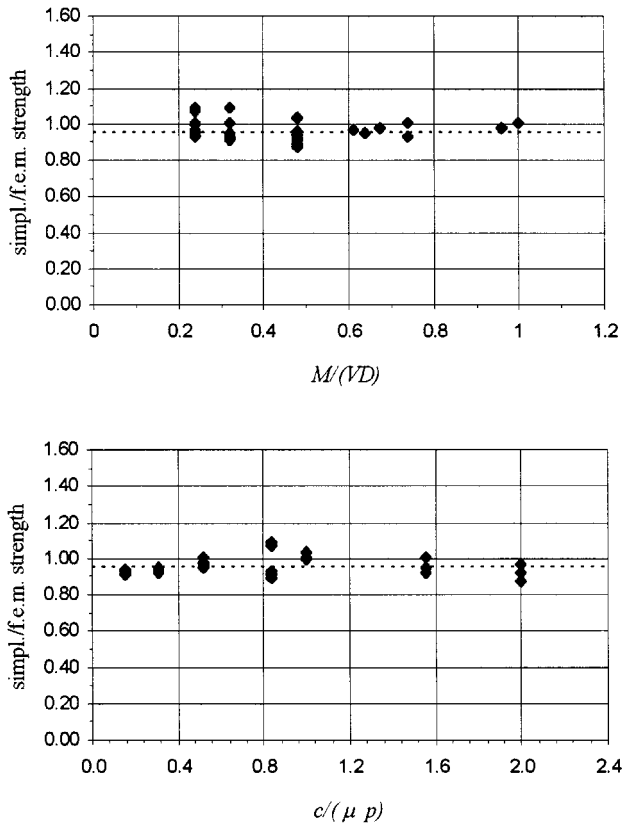

Figure 4. Comparison of the proposed simplified shear strength prediction formulae (equation (9)) with the strengths obtained from f.e.m. simulations of shear tests of walls. Mean simpl./f.e.m. strength = 0·964, standard dev. = 0·053

the case I of Figure 2, equation (9c) governed for cases similar to case II of Figure 2, while for mixed mechanisms the strengths given by equations (9b) and (9c) were close.

However, for the application of the proposed strength criterion to real walls, two considerations must be made.

First, the constitutive model used in the finite element simulation idealizes masonry as a layered material, made by the superposition of continuous, homogeneous layers of solid clay and mortar, thus neglecting the influence of headjoints. For this reason, the use of the local bedjoint strength parameters c and μ in equations (9) can reproduce fairly well the strength obtained from the finite element simulations: the transition from local failure conditions to the global strength of the wall is accounted for by the coefficients of equations (9b) and (9c), which depend primarily on the shear ratio. However, in real brickwork, due to the presence of headjoints, the direct use in equation (9) of the bedjoint cohesion and coefficient of friction, as derived from laboratory or *in situ* tests, could easily lead to an overestimatation of the real strength of a wall. The role of weak headjoints and a possible correction of the cohesion and friction coefficient was discussed by Mann and Müller.[14] According to their model, a corrected cohesion and coefficient of friction are expressed as $\bar{c} = \kappa c$, $\bar{\mu} = \kappa\mu$, where

$$\kappa = \frac{1}{1 + \mu 2\Delta_y/\Delta_x} \tag{10}$$

and Δ_x, Δ_y, respectively are the length and height of the brick unit. Such a correction is recommended when using equation (9).

A second important consideration is that equation (9) accounts only for shear failures governed by joint failures, while experiments show that in presence of high axial loads or strong mortar the failure may be initiated by shear-tensile cracking of bricks. Again, a possible formulation of the local shear strength based on cracking of bricks, given the tensile strength of bricks f_{bt}, can be found in Mann and Müller:[14]

$$\tau_{u,b} = \frac{f_{bt}}{2{\cdot}3}\sqrt{1 + \frac{\sigma_v}{f_{bt}}} \tag{11}$$

By putting $\sigma_v = p = P/(Dt)$ and introducing a correction factor to take into account the influence of aspect ratio, similarly to what proposed for joint failures, the local criterion expressed by equation (11) can be transfomed into a global strength criterion as

$$V_{d,b} = Dt\,\tau_b = Dt\,\frac{f_{bt}}{2{\cdot}3(1 + \alpha_V)}\sqrt{1 + \frac{p}{f_{bt}}} \tag{12}$$

where the proposed correction coefficient $(1 + \alpha_V)$ encompasses the effects of complex stress distribution, crack propagation and shear–flexure interaction.

The shear strength of a wall should then be calculated as the lowest strength obtained from equations (9) and (12). In the following the discussion on shear strength will continue on the basis of experimental results.

2.3. Experimental results

In recent years a co-ordinated research effort among several research institutions[12,13] has led to extensive experimental and numerical research on the behaviour of unreinforced brick masonry. Among the tests performed, cyclic shear tests on walls with different aspect ratio and different axial load level were performed,[1,2] together with a rather detailed study of the separate material components: bricks, mortar, mortar joints.[15] Two separate series of static tests on walls are considered here: one performed at the University of Pavia[2] and one performed at the Joint Reserch Centre of the European Community in Ispra.[1] The material properties are summarized in Table I for the two separate series of walls and are described in more detail elsewhere.[2,15] The shear tests on brick-mortar joints were performed on triplets and the results are reported in terms of cohesion and friction obtained from a linear regression on the data points (maximum

Table I. Material properties for the shear tests on walls performed in Pavia and in Ispra

Property	Symbol	Pavia tests		Ispra tests	
		Mean	c.o.v. (%)	Mean	c.o.v. (%)
Brick tensile strength	f_{bt}	1·26 MPa (1)	20·3	2·44 MPa (2)	25·8
Brick compression strength (flatwise)	f_b	19·7 MPa	8·8	26·9 MPa	9·0
Mortar compression strength	f_m	4·33 MPa	1·8	3·31 MPa	10·6
Mortar tensile strength (Bending test)	f_{mt}	1·59 MPa	3·5	0·58 MPa	25·8
Joint tensile strength	f_{jt}	0·07 MPa	10·5	0·04 MPa	25·7
Joint cohesion (3)	c	0·21 MPa	49·0	0·23	17·9
Joint coeff. of friction (3)	μ	0·81	—	0·58	—
Masonry compression strength	f_u	7·9 MPa	20·2	6·2 MPa	12·2
Brick nominal dimensions		55 mm × 120 mm × 250 mm			
Bedjoint nominal thickness		10 mm			
Mortar composition		Hydraulic lime/sand = 1/3 in volume			

Note: (1) splitting test on whole units; (2) bending tests on whole units; (3) obtained from shear tests on triplets

average shear stress vs. average compression stress). The materials of the tests performed in Ispra are the same as those used for a full scale building prototype tested in Pavia.[12,13,15] The walls in Pavia were three-wythes thick (380 mm), had a length of 1·5 m and a height of 2·0 or 3·0 m. They were built with alternate courses of stretchers and headers (English bond). A total of five walls were tested under cyclic shear in a static testing frame at different levels of vertical load. The tests were made keeping the top and the bottom wall sections parallel. Similar tests were performed in Ispra on four smaller walls which were two-wythes thick (250 mm), had a length of 1·0 m and a height of 1·35 or 2 m, keeping thus the same aspect ratios as in the Pavia tests. In the Ispra tests, servo-controlled actuators kept the vertical load constant and the top base parallel to the bottom base while the horizontal displacement at the top was increased. Small variations of the vertical load took place during the tests on the bigger walls in Pavia, where a higher load capacity was available but static electro-hydraulic valves made a perfect control of the vertical load difficult.

All tests were cyclic, with the exception of one monotonic (Pavia, wall MI1 m). The tests showed:

(1) diagonal cracking with prevailing joint failure for the lower values of axial load ($p = 0{\cdot}6$–$0{\cdot}7$ MPa) and aspect ratio ($H/D = 1{\cdot}35$);
(2) cracking of bricks for the higher values of axial load ($p = 1{\cdot}0$–$1{\cdot}2$ MPa) and aspect ratio ($H/D = 2{\cdot}0$);
(3) mixed joint and brick failure for intermediate combinations of the parameters.

The proposed strength formulae (equations (9) and (12)) were checked against the experimental strengths. In these comparisons, the mean cohesion and friction coefficients reported in Table I were corrected according to Mann and Müller (equation (10)), and were then inserted in equation (9). Since the walls were all built in English bond (alternate stretcher and header courses) the value of Δ_x was taken as the mean between the stretcher (250 mm) and the header (120 mm). Besides cohesion and friction of the bedjoint, an additional parameter needed is the direct tensile strength of the bricks (equation (12)). The problems in measuring experimentally the direct tensile strength of the bricks are the same as for concrete or lithic materials. The most common methods are indirect methods such as the splitting test (relevant to the Pavia tests) and the bending test (relevant to the Ispra tests). The correction coefficient 0·85 was applied to the strength obtained from the splitting test, and the correction coefficient 0·5 was applied to the strength obtained from the bending test (modulus of rupture), to obtain the direct tensile strength. Both coefficients were chosen on the basis of known existing experimental correlations for concrete specimens. Although no extensive experimental database is available yet for clay bricks to check these coefficients, the experiments performed at the Politecnico of Milano[15] on the materials used for the Ispra tests and for the construction of a building prototype tested in Pavia, show that these coefficients are acceptable also for the tests made on solid clay bricks. All the corrected values of the parameters used for the application of equations (9) and (12) are summarized in Table II.

The strength predictions (Figure 5) appear to be satisfactory, slightly conservative (mean value of predicted/experimental strength = 0·85), and consistent with the failure modes which were experimentally

Table II. Parameters used for the simplified strength calculations for the shear tests on walls performed in Pavia and in Ispra

Property	Symbol	Pavia tests	Ispra tests
Corrected joint cohesion (1)	$\bar{c}$	0·14 MPa	0·17 MPa
Corrected joint coeff. of friction (1)	$\bar{\mu}$	0·55	0·43
Brick direct tensile strength	f_{bt}	1·07 MPa	1·22 MPa

Note: (1) correction according to equation (10) with $\Delta_x = 185$ mm, $\Delta_y = 55$ mm

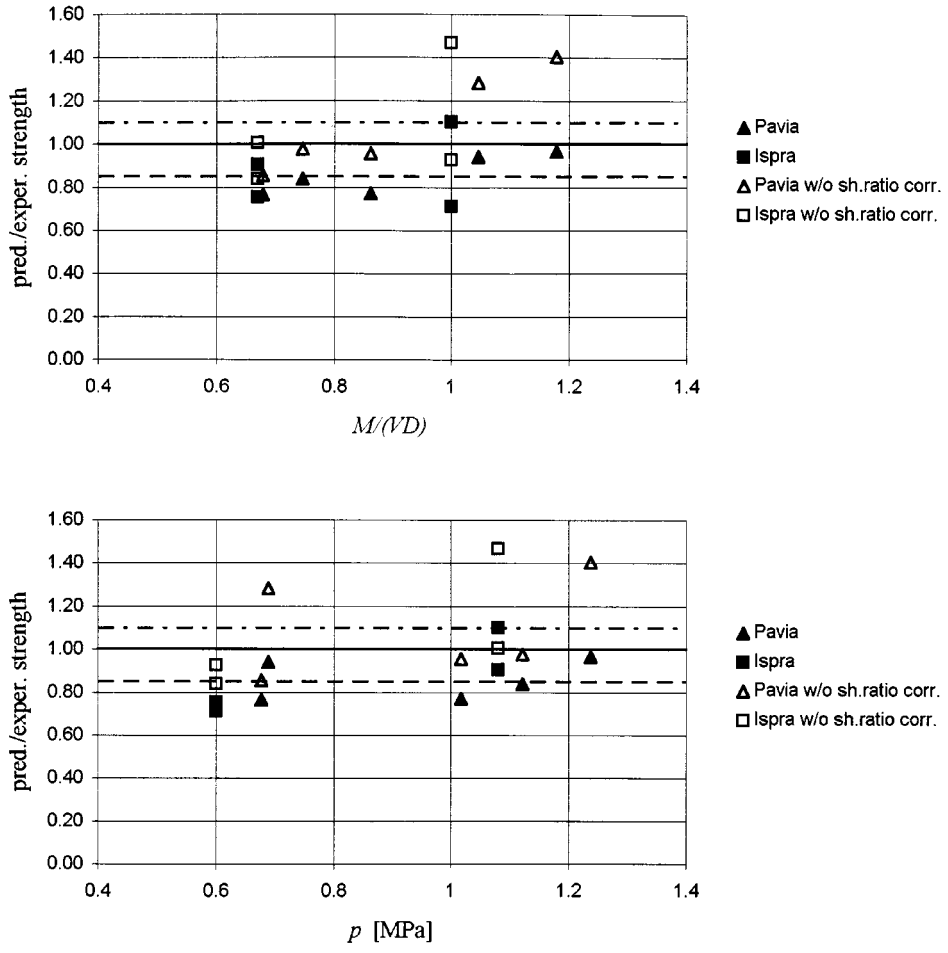

Figure 5. Comparison of the simplified shear strength prediction formulae with measured experimental strengths in the tests performed in Pavia and Ispra. As proposed (equations (9) and (12)): mean pred./exper. strength = 0·85 (dashed line), standard dev. = 0·12. Without shear ratio correction: mean pred./exper. strength = 1·10 (dash-dotted line), standard dev. = 0.24

reported: equation (9c) was governing for the cases with observed prevailing joint failure and equation (12) was governing for prevailing brick failure. The scatter between experiment and prediction (standard deviation = 0·12) is higher than in the case where comparison is made with respect to finite element simulations, as it can be expected for experimental behaviour. However, the scatter is comparable with the scatter of the mechanical properties of masonry. To show the effectiveness the correction factor $(1 + \alpha_V)$ in equations (9c) and (12), Figure 5 reports also the results which could be obtained by substituting the factor $(1 + \alpha_V)$ with a constant value of 1·5, consistent with the assumption of a parabolic distribution of shear stresses along the uncracked section. As it can be seen, the scatter is doubled (standard deviation = 0·24) and there is a clear trend in the predictions to be unconservative as the shear ratio increases. This is in agreement with what suggested by the nonlinear finite element simulations.

The proposed simplified shear strength formulae can be considered appropriate for the range of parameters considered in the presented numerical and experimental investigations. In particular, the values of shear ratio α_V ranged up to 1·2. It must be considered, however, that for values of α_V greater than 1·5, and for

the levels of mean normal stress p commonly present in masonry buildings, shear failures tend to be superseded by rocking (flexural failures). A limitation to the correction factor $(1 + \alpha_V) \leqslant 2{\cdot}5$ is suggested. Further experimental comparisons are needed to check the validity of the proposed formulae for a broader range of parameters, although the range considered herein covers large part of the cases of practical interest.

3. DEFORMATION CAPACITY AND STIFFNESS EVALUATION

Response of brick masonry walls is strongly nonlinear also at low level of load, due to the low tensile strength of bed and headjoints. As the damage due to cracking increases, masonry walls show both strength and stiffness degradation. A definition of elastic stiffness of a wall subjected to in-plane shear must therefore be related to a reference stress or deformation. A common approach followed for design and assessment purposes is to idealize the cyclic envelope with a bilinear curve. In Figure 6, a possible definition of the parameters of the bilinear curve is given. The ultimate displacement δ_u corresponds to a specified limit to strength degradation. The initial elastic stiffness and the value of V_u should be such that the bilinear curve is equivalent in an energetic sense to the experimental envelope. A possible choice for the initial stiffness is the secant stiffness at $0{\cdot}75\,V_u$.[16] Studies performed in Ljubljana (Slovenia) by Tomazevic *et al.*[17] have shown that the choice $V_u = 0{\cdot}9\,V_{max}$ is appropriate for energy equivalence in masonry walls failing in shear. The envelope, or skeleton curve is actually dependent on the type of loading history, (e.g. monotonic or cyclic, quasi-static or dynamic, and sequence of cycles) especially when shear failures are involved, and this constitutes a problem for the correlation of different experimental procedures. The data examined here refer to the abovementioned tests (Section 2.3), which are all quasi-static cyclic, with reversed cycles of increasing imposed displacement, with the exception of two pseudo-dynamic tests (from the Ispra tests[1]).

3.1. Flexural response

In case of a pure flexural response, i.e. of a potential rocking response, very large displacements can theoretically be obtained without significant loss in strength, especially when the mean axial load is low compared to the compressive strength of masonry. A typical flexural response is depicted in Figure 7, case A, where a very moderate hysteretic energy dissipation and an almost nonlinear elastic behaviour is shown, with negligible strength degradation in subsequent cycles at the same peak displacement. If no other failure mechanism occurs, the displacements which can be attained in a rocking response can be limited only by a decrease in strength due to second order $(P - \Delta)$ effects associated with overturning. These limits can be as high as 10 per cent of the height of the wall and are of no practical use, since other collapse events will always take place before reaching this drift limit. As a consequence neither an ultimate displacement nor a secant stiffness to collapse can be defined for this response mode. Both values will depend on the demand from the seismic input or from the limit imposed by other failure modes.

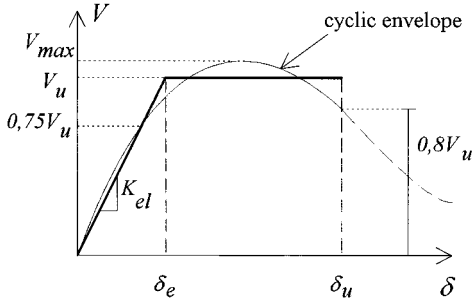

Figure 6. Definition of an equivalent bilinear envelope. $V_u = 0{\cdot}9\ V_{max}$ for shear failure

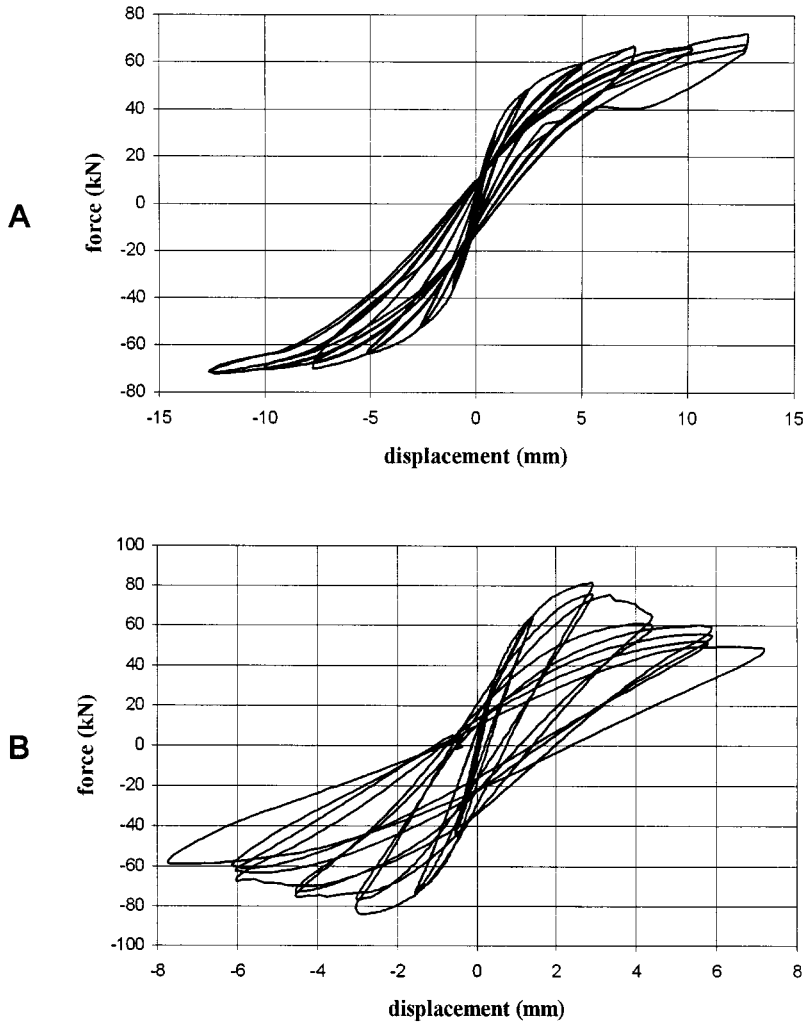

Figure 7. Experimental behaviour of simple piers, fixed–fixed conditions. (A) example of flexural response, $H/D = 2$, $p = 0{\cdot}6$ MPa. (B) example of behaviour with diagonal shear cracking, $H/D = 1{\cdot}35$, $p = 0{\cdot}6$ MPa (Reference 1)

3.2. Diagonal shear cracking response

A typical force–displacement curve in case of a response dominated by shear cracking is shown in case B of Figure 7. Most of the tests considered here showed such a kind of failure, and observation of the experimental results allowed the following comments.

The pre-cracking behaviour was characterized by moderate hysteresis, and by negligible strength and stiffness degradation. Initiation of the first visible diagonal cracks corresponded to a force which was at least 90 per cent of the peak lateral force. Post-peak response was characterized by higher energy dissipation but by rather rapid strength and stiffness degradation.

For all the considered tests an equivalent bilinear curve was defined according to Figure 6, where the ultimate displacement is defined as the displacement corresponding to a strength degradation of 20 per cent

Table III. Ultimate drift and ductility associated to shear failure from experimental quasi-static tests (fixed–fixed boundary condition)

Monotonic test				
Wall	H/D	p (MPa)	δ_u/H	δ_u/δ_e
MI1 m	1·33	1·02	$8{\cdot}75\times10^{-3}$	5·47
Cyclic tests				
Wall	H/D	p (MPa)	δ_u/H	δ_u/δ_e
MI1 (+)	1·33	1·12	$5{\cdot}10\times10^{-3}$	4·25
MI2 (−)	1·33	0·68	$5{\cdot}95\times10^{-3}$	2·53
MI3 (+)	2·00	1·24	$4{\cdot}80\times10^{-3}$	3·27
MI3 (−)	2·00	1·24	$4{\cdot}93\times10^{-3}$	4·63
MI4 (+)	2·00	0·69	$5{\cdot}00\times10^{-3}$	1·83
MI4 (−)	2·00	0·69	$6{\cdot}00\times10^{-3}$	2·28
ISP1 (+)	1·35	0·60	$4{\cdot}37\times10^{-3}$	4·54
ISP1 (−)	1·35	0·60	$5{\cdot}41\times10^{-3}$	7·30
ISP3 (+)	1·35	1·08	$5{\cdot}26\times10^{-3}$	6·45
ISP3 (−)	1·35	1·08	$6{\cdot}15\times10^{-3}$	7·55
		mean	$5{\cdot}30\times10^{-3}$	4·46
		c.o.v. (%)	10·90	46·30

Note: MI: tests performed in Pavia; ISP: tests performed in Ispra; (+), (−) respectively positive, negative direction

below the ultimate strength V_u (28 per cent below V_{max}). Since the number of repetitions of the cycles at the peak displacement was not the same for all the tests, the reference envelope was evaluated for each wall considering the peaks at the first cycle for a given displacement level (first cycle envelope). The results were examined in terms of 'yield' displacement δ_e, and consequently of initial stiffness $K_{el} = V_u/\delta_e$, of ultimate displacement δ_u, and ductility δ_u/δ_e. It was found that the evaluation of an equivalent yield point presents a large dispersion, and its variation is not apparently correlated in a consistent way with, say, axial load or slenderness, although physical considerations call for an increase in stiffness with increasing mean axial load and a decrease in stiffness with increasing slenderness. The same could be said for the calculated drift (yield displacement divided by wall height) at yield.

On the other hand, the drift at ultimate conditions (δ_u/H) was found to be extraordinarily uniform, as shown in Table III, with a mean value of $5{\cdot}3\times10^{-3}$ and a coefficient of variation of 10 per cent. In the same table it can be seen how the scatter in the displacement at yield is reflected in the scatter of the measure of ductility. A possible explanation for this result is that, since the initial elastic stiffness is associated with a branch where crack initiation and propagation is dominating on the tensile side, and mortar compaction on the compressive side, high scatter is reported in initial stiffness evaluation. On the other hand, since the ultimate drift is associated with friction and interlocking mechanisms in stabilized cracks which increase in size (opening), the scatter is reduced. Ultimate drift appears therefore as a more reliable parameter than ductility. When ultimate conditions are considered, strength and ultimate displacement are the dominating parameters, and the determination of the initial elastic stiffness plays a lesser role. The definition of a strength (Section 2) and of an ultimate displacement allows an easy definition of a secant stiffness to ultimate conditions $K_s = V_u/\delta_u$.

3.3. Sliding shear response

When sliding on horizontal bedjoints occur, a very stable mechanism is involved, since high displacements are possible without the a loss of integrity of the wall. Damage and dissipation are concentrated in a bedjoint, and as long as a vertical load is present, high energy dissipation is possible, as shown by cyclic tests on bedjoints.[18] Dynamic tests on walls[19] showed that rocking and sliding typically take place together, when low axial loads are present. An ultimate displacement limit for sliding has, as in the case of rocking, no real meaning since it would be so high that the occurrence of other failures would in practice determine the real displacement limit.

4. ENERGY DISSIPATION CAPACITY EVALUATION

4.1. Flexural response

The hysteretic energy dissipated in a typical rocking mode response is generally small, as shown in Figure 7. In this context the dissipated hysteretic energy will be examined in terms of equivalent viscous damping, which, given a single load–displacement cycle can be expressed as a function of the dissipated energy W_d and the elastic energy at peak displacement W_e: $\xi_{eq} = W_d/2\pi(W_e^+ + W_e^-)$. Typically, the dissipated energy in each cycle evolves with the increase of damage and with the increase of displacement demand. The values of equivalent damping obtained calculating the area of each single cycle from the test in Figure 7, case A, are shown in Figure 8 as a function of drift, and have a mean value of 5·3 per cent. In dynamic conditions, when rocking occurs, however, an additional energy dissipation mechanism is given by impact and radiation damping. If the viscous damping equivalent to the energy dissipated by perfect inelastic impact on the soil is evaluated using the simplified approach of Housner,[20,21] some useful indications can be obtained. If the mass of the wall can be neglected with respect to the supported mass, and all the mass is supposed concentrated at the top of the wall, it is possible to derive the following expression for the equivalent damping corresponding to impact:

$$\xi_e = 48\ [1 - (\cos 2\theta)^2] \tag{13}$$

where θ is the angle between the vertical axis and the line connecting the central point of the top of the wall and the edge point of the base. This equation allows an estimate of the equivalent damping as a function of the geometry of the wall only. It is found that the equivalent radiation damping can be significant, and increases rapidly as the wall gets squatter. However, rocking is likely to occur for slender walls. If a wall with aspect ratio $H/D = 3{\cdot}0$ in single bending is considered ($\tan\theta = 1/6$), a value of $\xi_e = 5{\cdot}4$ per cent would result. This value can be considered as a good low bound reference, since the slenderness ratio of 3·0 can be considered as an upper limit for walls which can be taken into consideration for seismic resistance. Although this quantification is very rough, it is believed that a 5 per cent equivalent impact damping is a minimum which can be safely used in addition to viscous and hysteretic damping for an equivalent linear dynamic analysis. It appears therefore that for limit cases of rocking mode, approximate values of the global equivalent viscous damping associated to hysteresis and radiation damping can be 10 per cent, in addition to the default viscous damping (5 per cent for Eurocode 8[22]) used for linear response analysis.

4.2. Diagonal shear cracking response

The hysteretic energy dissipation capacity of a diagonal shear response was evaluated in terms of equivalent viscous damping. In Figure 8 the equivalent damping is also shown for the wall of Figure 7, case B. A clear trend to an increase in dissipation after diagonal cracking is apparent. The hysteretic energy content of each cycle is approximately constant after cracking, independent of displacement or ductility, with the exception of the first cycle to a significantly larger drift. It can be noted that before diagonal cracking the equivalent damping is very close to the value reported for rocking response.

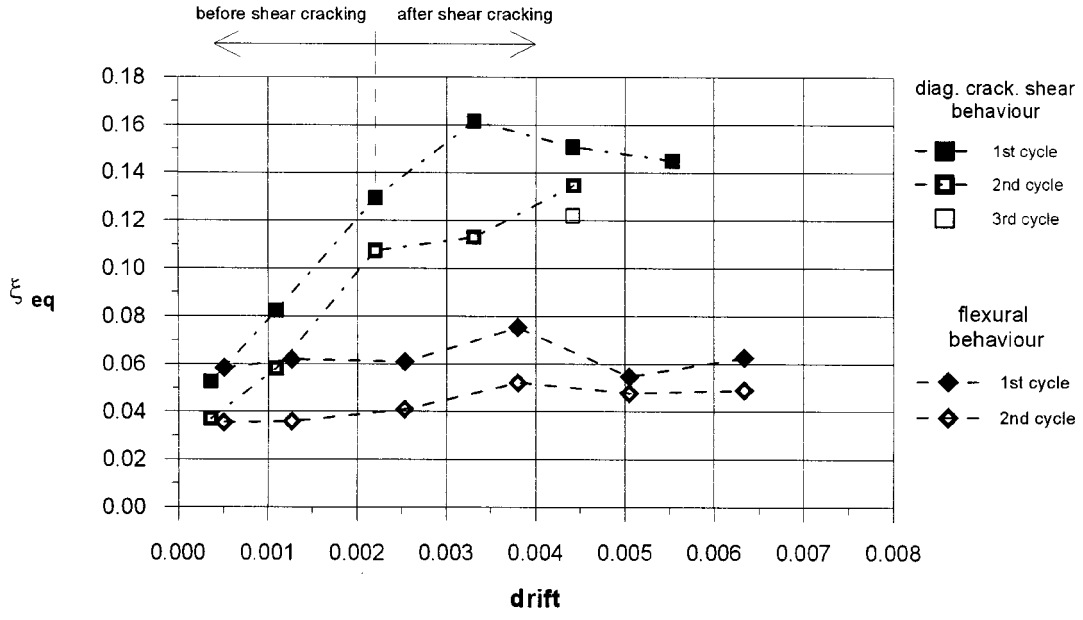

Figure 8. Equivalent hysteretic damping from the cyclic tests of Figure 7 (flexural and diagonal shear cracking behaviour)

Table IV. Equivalent damping evaluated from hysteretic energy dissipation. For walls with shear failure equivalent damping is evaluated after shear cracking

Failure mode	Mean	c.o.v. (%)
Shear failure, cyclic test	0·133	14·1
Shear failure, pseudo-dynamic test	0·099	46·1
Mixed flexural-shear, cyclic test	0·065	16·3
Flexural (rocking), cyclic test	0·053	22·4

If a pseudo-dynamic test is considered, which was the result of a sequence of several accelerograms of increased intensity applied to the wall,[1] lower values of equivalent damping are reported (Table IV). In such a case, a very high amount of hysteretic energy is dissipated in one cycle just immediately after diagonal cracking, while the remaining cycles tend to show lower dissipation (this also explains the higher coefficient of variation of the calculated equivalent damping). However, the number of cycles to which the wall was subjected in the pseudo-dynamic test, as a sequence of six accelerograms, was very high and the total energy dissipated in such a test was approximately twice the amount dissipated in the cyclic test. As a consequence, much higher degradation of internal friction mechanisms was generated. Given the results of the cyclic and pseudodynamic tests, a value of $\xi_e = 10$ per cent could be considered as appropriate for post-cracking behaviour of diagonal shear failure modes.

Table IV reports also the equivalent damping calculated from a wall failing in a mixed shear-flexural mechanism, after shear cracks have formed ($p = 0{\cdot}8$ MPa, $H/D = 2{\cdot}0$). The moderate energy dissipation is due to the pinching effect given by the superposition of the rocking-flexural deformation to the shear

deformation. Such a case is typical of situations when the calculated flexural strength of the wall is very close to the shear strength. In such cases the equivalent damping typical of flexural response appears to be a conservative reference.

4.3. Shear sliding response

As the pure shear sliding cyclic response is very close to an indefinitely elastic perfectly plastic response, equivalent damping evaluation would lead to very high values of ξ_e, with an asymptotic value of 64 per cent for indefinitely large displacements. None of the quasi static experiments carried out in this research showed a pure sliding failure mechanism. Also in the dynamic experiments described in Reference 19 sliding was accompanied or followed either by rocking or diagonal cracking. It would be therefore very unconservative, in an assessment procedure like that proposed in the following section, to assume such a high-energy dissipation capacity, particularly since our ability to predict the failure mechanism is based on approximated strength evaluations. At present no clear experimental information is available on the contribution of sliding to energy dissipation in these mixed-mode or transition situations. In absence of such a reference, special caution should be used for the definition of equivalent damping values in excess of what can be assumed for rocking or diagonal shear cracking.

5. A SIMPLE ASSESSMENT APPROACH

5.1. Equivalent structure

The assessment procedure presented herein has mainly a conceptual and methodological value, since it is at present applicable only to ideal, simple, one-degree-of-freedom systems, and it is not yet fully applicable to real buildings, since the phenomena related to interaction between different walls and other structural and non-structural elements have not been considered. Furthermore, the assessment concepts presented here need to be extended to multi-degree-of freedom systems and complex structures. These aspects are presently being investigated.

The assessment approach described in the following is based on the definition of a substitute structure model, where the true non-linear response is simulated with a linear model with appropriate equivalent stiffness and viscous damping, according to an approach proposed for concrete structures by Shibata and Sozen.[23] The equivalent effective damping of a system is obtained from consideration of an assumed hysteretic response at a specific level of displacement or drift. The effective period of vibration of a system is assumed to be the period at maximum response, and consequently the effective stiffness is assumed to be the secant stiffness to maximum response, as shown in Figure 9 (and putting $V_e = V_u$). The main objective of the assessment is to evaluate the multiplier of the peak ground acceleration inducing the ultimate limit state (i.e. inducing the conventional collapse), rather than computing the displacement induced by a given input

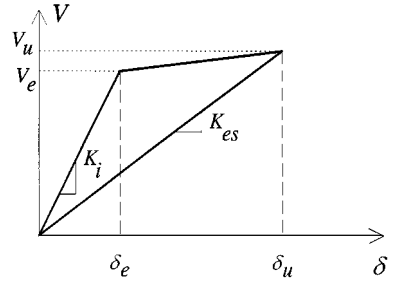

Figure 9. Equivalent secant stiffness for the substitute structure at ultimate conditions (general case with $V_e \neq V_u$)

motion. It is therefore consistent to assume that the maximum displacement will be attained. Both effective stiffness and effective viscous damping have to be adjusted so that the displacement of the inelastic prototype is the same as the displacement of the linear substitute model for the given level of input. It has been discussed in Section 4 how the equivalent damping is not strongly affected by the input level, and essentially constant values can be adopted provided that some post-elastic mechanism will be induced. On the contrary, an appropriate adjustment of the model displacement is fundamental, since for the equivalent linear model different forces correspond to different displacements, while for the real structure the force is essentially constant after the equivalent yield level.

The substitute structure of a masonry wall should be identified recognizing first its failure mode, as the one corresponding to the lowest strength, and consequently evaluating its deformation and energy dissipation capacity.

In case of a *flexural* (*rocking*) failure mode, the strength can be computed according to equation (1), the viscous damping equivalent to the energy dissipated by impact depends on the aspect ratio of the wall (see equation (13)), and the ultimate drift is so large to be of no practical interest. A value of 15 per cent total equivalent damping can be adopted for assessment purpose, as discussed in Section 4·1, while considering that the non-structural damage is essentially increasing with the drift, a practical limit for the ultimate drift can be selected. A value equal to 1 per cent seems reasonable to the authors of this paper.

For the case of a *diagonal cracking shear* failure mode, the strength will be computed according to equations (9) and (12), a constant equivalent viscous damping equal to 15 per cent and a ultimate drift equal to 0·5 per cent will be assumed. In a previous section it has been shown that the value of the ultimate drift is much more stable than the value of an estimated ductility capacity, which is not required for the definition of the equivalent model.

When a *shear sliding* failure mode is assessed according to equation (8), the maximum drift is again too large to be of practical interest and again a limit of 1 per cent is suggested, and the energy dissipation capacity is conservatively assumed equal to 20 per cent, to consider possible mixed collapse modes.

Having defined strength and ultimate displacement, the secant stiffness of the substitute model and the corresponding period of vibration can be computed. For each one of the failure modes the real dynamic response will therefore be simulated using a linear model characterized by appropriate period of vibration and equivalent damping.

5.2. Seismic input

The earthquake input will be represented using either acceleration or displacement response spectra, characterized by different peak ground acceleration levels (Figure 10). The appropriate equivalent viscous damping (depending on the assessed failure mode) will be used, scaling the 5 per cent damping spectrum with the factor suggested in Eurocode 8:

$$\eta = [7/(2 + \xi)]^{1/2} \tag{14}$$

In case of a 15 per cent equivalent viscous damping this factor is equal to 0·64. If the variation of the period of vibration (from the initial stiffness to the secant stiffness to the ultimate displacement) does not contribute to a variation of the spectral acceleration (e.g., for the spectral shape defined in the EC8, the period corresponding to the secant stiffness is not larger than 0·4, 0·6 or 0·8 s depending on the soil properties), the force reduction factor can be obtained as the reciprocal of η ($q = 1/\eta$, using the EC8 notation). In this case therefore a scaling factor η equal to 0·64 corresponds to a force reduction factor equal to 1·56; larger q-factors would be obtained if the period shift induced a reduction of the spectral acceleration.

Similarly, a force reduction factor equal to 1·77 can be computed if the equivalent damping is equal to 20 per cent and there is no spectral acceleration reduction due to period elongation.

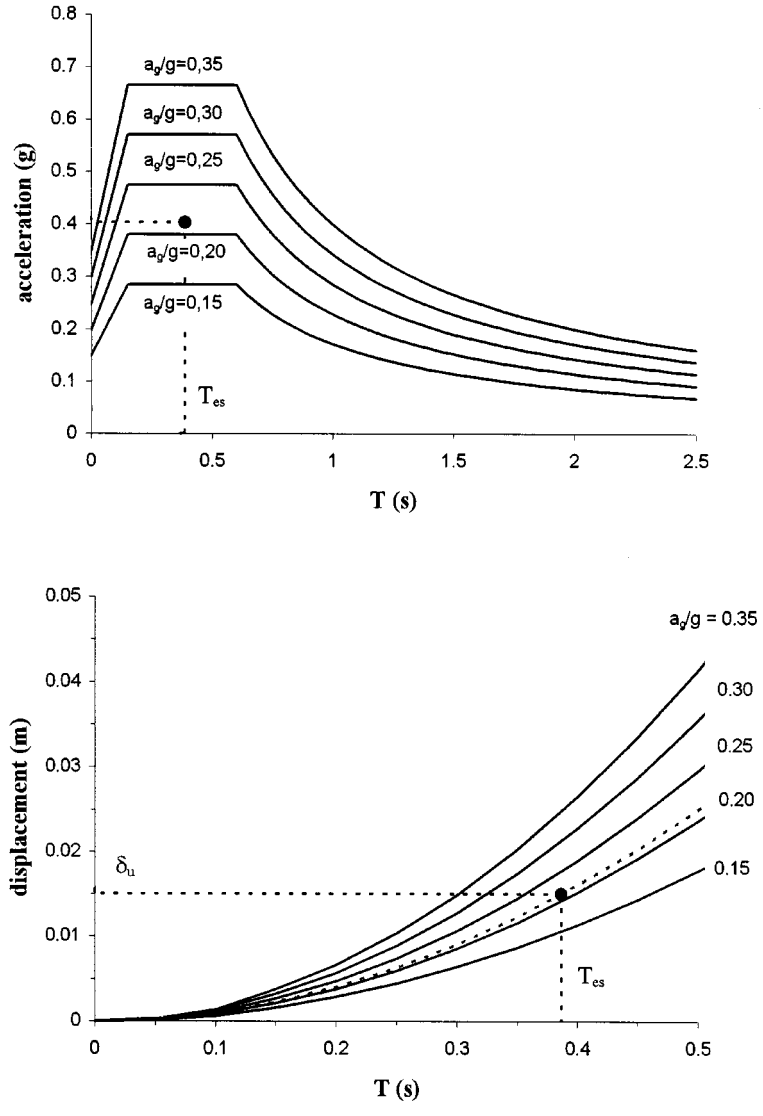

Figure 10. Design acceleration and displacement response spectra (from EC8, soil type B)

5.3. Assessment procedure

The equivalent structures defined in Section 5·1 are conceptually different from analogous models used for reinforced concrete structure, essentially because the equivalent damping can be computed a priori, and does not depend on the response, as discussed in Section 4. A second important difference is due to the usually high stiffness of masonry structures, which results in rather low periods of vibration, even considering the secant stiffness to failure.

As a consequence in most cases (particularly in case of shear failure) the period of vibration of the structure will correspond to the region of maximum amplification of the acceleration spectrum, as in the case of the example indicated in Figure 10. Either the displacement or the acceleration spectrum can be entered, both

with the period of vibration of the equivalent structure and with the ultimate displacement or the acceleration corresponding to the model strength, to read off the ground acceleration level that can be taken by the wall without failure.

It is obvious that the larger drift allowed for flexural or shear sliding response and the larger energy dissipation capacity of this last failure mode, makes these failure modes particularly attractive in comparison with any kind of shear failure, as defined by equations (9) and (12). It is therefore safer to predict a shear failure when the force required to induce different failure modes are similar. The probability of a shear failure increases for larger values of the axial load, which therefore do not necessarily correspond to safer structures, even when the shear strength is higher. When uncertainties on the real vertical load exist it is recommend to verify different situations and assume the lower ground acceleration coefficient. It is also possible to see that a diagonal cracking failure is very unlikely for slender walls (e.g. shear ratio above 1.5). Unfortunately most existing masonry walls fall below such a value of shear ratio and are dominated by diagonal cracking.

6. CONCLUSIONS

The results presented in this paper were focused on some fundamental issues of interest for the seismic assessment of masonry walls subjected to in-plane action.

First, the issue of strength evaluation was considered, with special attention to shear strength, where numerical and experimental tests were used to show the role played by the shear ratio and to define a simplified formulation for shear strength, with simple modification of existing criteria.

Subsequently, the deformation and energy dissipation capacity of walls were discussed on the basis of experimental results. The following conclusions summarize the main results, considering the case of flexural, diagonal shear cracking and sliding failure.

Diagonal shear cracking failure

(a) the evaluation of the strength requires the consideration of different possible failure mechanisms and is controlled also by the value of the shear ratio, due to the interaction with flexure; the proposed simplified formulae accounting for joint or brick failure and for whole or cracked section failure, were shown to give satisfactory results within the range of parameters investigated herein;
(b) for the masonry material considered in this paper, the ultimate deformation capacity in shear is very stable when expressed in terms of drift and corresponds approximately to 0·5 per cent
(c) on the contrary a quantification of ductility in terms of ultimate/yield displacement ratio is highly scattered, even considering walls built with the same material;
(d) the ratio between the energy dissipated in each cycle and the elastic strain energy absorbed at maximum displacement remains approximately constant with increasing drift, with an equivalent viscous damping which can be safely estimated around 10 per cent;

Flexural failure

(a) existing formulae for strength evaluation are simple and reliable;
(b) large energy dissipation capacities are potentially available through a rocking mechanism, but the available experimental results do not allow yet a reliable evaluation; a total equivalent viscous damping of 15 per cent can be safely adopted, and the choice was justified in the paper;
(c) large deformation capacity is available; an ultimate drift level equal to 1 per cent is recommended for the sole purpose of nonstructural damage limitation.

Sliding failure

(a) extremely large energy dissipation capacities are theoretically available;
(b) however, available experiments show that sliding can intervene as an additional dissipation mechanism together with other failure modes (rocking or diagonal cracking), but pure sliding behaviour was not observed. No clear reference is available yet for quantification of equivalent damping.
(c) again,a large deformation capacity is available and a practical limit value of 1 per cent is recommended.

The assessment procedure presented in the final sections of the paper, based on a substitute structure approach, has mainly a conceptual and methodological value. Extension is needed to multi-degrees-of-freedom systems and complex structures. These aspects are presently being investigated. The conceptual value of the proposed procedure consists essentially in the inclusion of deformation and energy dissipation capacity of the expected failure mode in the evaluation of the ground acceleration corresponding to collapse. Actually in the present state of practice the strength is computed and a force reduction factor (1·5 is a commonly recommended value for unreinforced masonry structures[22]), independent of the potential collapse mode, is applied to take into account the nonlinear response. This may result in non uniform levels of protection against different modes of collapse, if the failure modes have different energy dissipation capacity. The experimental and analytical results presented in this paper seem to confirm that a force reduction factor equal to 1·5 is a sound conservative value to be used in a standard strength-based evaluation of the seismic response. Nevertheless, significant differences may result from the application of the proposed assessment approach, particularly when whole buildings should be considered, due to the combined effects of post-elastic mechanisms, equivalent damping and period shift.

ACKNOWLEDGEMENTS

Funding from C.N.R., Gruppo Nazionale per la Difesa dai Terremoti (Italian National Research Council, National Group for the Protection from Earthquakes) is gratefully acknowledged.

REFERENCES

1. A. Anthoine, G. Magenes and G. Magonette, 'Shear compression testing and analysis of brick masonry walls', *Proc. 10th European Conference on Earthquake Engng*., Vienna, 1994, pp. 1657–1662.
2. G. Magenes and G. M. Calvi, 'Cyclic behaviour of brick masonry walls', *Proc. of the 10th World Conference on Earthquake Engng*., Madrid, 1992, pp. 3517–3522.
3. D. P. Abrams, 'Strength and behavior of unreinforced masonry elements', *Proc. 10th World Conference on Earthquake Engng*., Madrid, 1992, pp. 3475–3480.
4. M. Tomazevic, 'Masonry structures in seismic areas — a state-of-the-art report', *9th European Conference on Earthq. Engng*., Moscow, 1990, Vol. A, pp. 246–302.
5. V. Turnšek and P. Sheppard, 'The shear and flexural resistance of masonry walls', *Proc. Intern. Research Conference on Earthq. Engng*., Skopje, 1980, pp. 517–573.
6. V. Turnšek and F. Cacovic, 'Some experimental results on the strength of brick masonry walls', *Proc. of the 2nd Int. Brick Masonry Conference*, Stoke-on-Trent, 1971, pp. 149–156.
7. D. Benedetti and M. Tomazevic, 'Sulla verifica sismica di costruzioni in muratura (on the seismic assessment of masonry structures)', *Ingegneria Sismica*, Vol. I, No. 0, 1984, pp. 9–16 (in Italian).
8. Eurocode 6, 'Design of masonry structures. Part 1-1: General rules for buildings. Rules for Reinforced and Unreinforced Masonry', ENV 1996-1-1, CEN, Brussels, 1994.
9. L. Gambarotta and S. Lagomarsino, 'Modeling unreinforced brick masonry wall', *Proc. U.S.–Italy Workshop on Guidelines for Seismic Evaluation and Rehabilitation of Unreinforced Masonry Buildings*, Pavia, *Technical Report NCEER-94-0021*, National Centre for Earthquake Engineering, Buffalo, 20 July 1994.
10. L. Gambarotta and S. Lagomarsino, 'Damage models for the seismic response of brick masonry shear walls. Part II: the continuum model and its applications', *Earthquake Engng. Struct. Dyn*., **26**, pp. 441–462 (1996).
11. ADINA R & D, '*ADINA — Automatic Dynamic Incremental Nonlinear Analysis*', *release 6.1*, Watertown, Massachusetts, U.S.A., 1995.
12. G.M. Calvi and G. Magenes, 'Experimental Research on Response of URM Building Systems', Proceedings of the U.S.–Italy Workshop on Guidelines for Seismic Evaluation and Rehabilitation of Unreinforced Masonry Buildings, Pavia, *Technical Report NCEER-94-0021*, National Centre for Earthquake Engineering, Buffalo, 20 July, 1994.

13. G. Magenes, G. M. Calvi and G. R. Kingsley, 'Seismic testing of a full-scale, two-story masonry building: test procedure and measured experimental response', in: *Experimental and Numerical Investigation on a brick Masonry Building Prototype - Numerical Prediction of the Experiment*, *Report 3·0 - G.N.D.T.*, Pavia, January 1995.
14. W. Mann and H. Müller, 'Failure of shear-stressed masonry — An enlarged theory, tests and application to shear walls', *Proc. British Ceramic Society*, No. 30, September 1982.
15. L. Binda, C. Tiraboschi, G. Mirabella Roberti, G. Baronio and G. Cardani, 'Measuring masonry material properties: detailed results from an extensive experimental research', *Experimental and Numerical Investigation on a brick Masonry Building Prototype*, *Report 5·0 - G.N.D.T.*, Milano, June 1995.
16. T. Paulay and M. J. N. Priestley, *Seismic Design of Reinforced Concrete and Masonry Buildings*, Wiley, New York, 1992.
17. M. Tomazevic, 'Recent advances in earthquake-resistant design of masonry buildings: European perspective', *Proc. 11th World Conference on Earthquake Engng.*, Acapulco, Paper No. 2012, 1996.
18. R. H. Atkinson, B. P. Amadei, S. Saeb and S. Sture, 'Response of Masonry Bed Joints in Direct Shear', *J. Struct. Div. ASCE*, **115**, 2276–2296 (1989).
19. G. Magenes and G. M. Calvi, 'Shaking table tests on brick masonry walls', *10th European Conf. Earthquake Engng*, Vienna, 1994, pp. 2419–2424.
20. G. W. Housner, 'The behaviour of inverted pendulum structures during earthquakes', *Bull. Seism. Soc. Am.*, **53**, 403–417 (1963).
21. M. J. N. Priestley, R. J. Evison and A. J. Carr, 'Seismic response of structures free to rock on their foundation', *Bull. New Zealand Soc. For Earthq. Engng.*, **11**, 141–150 (1978).
22. Eurocode 8 'Design provisions for earthquake resistance of structures. Part 1-1: general rules and rules for buildings — seismic actions and general requirements for structures', ENV 1998-1, CEN, Brussels, 1994.
23. A. Shibata and M. A. Sozen, 'Substitute-structure method for seismic design in R/C', *J. Struct. Div. ASCE* **102**, 1–18 (1976).

